Supplementary Information

Development of high stable Pt-based ORR catalyst over Mn-modified polyaniline-based carbon nanofiber

Jinghua Yu, [a] Qian Zhou, [a] Xiaoyi Xue, [c] Haitao Zhang, [b] Xiaojin Li, [d] Fanghui Wang, [a] Qingjun Chen, * [bcd] and Hong Zhu *[a]

[a]*State Key Laboratory of Chemical Resource Engineering Institute of Modern Catalysis, Department of Organic Chemistry, College of Chemistry, Beijing University of Chemical Technology Beijing, 100029 China*

[b]*CAS Key Laboratory of Green Process and Engineering Beijing Key Laboratory of Ionic Liquids Clean Process Chinese Academy of Sciences Beijing, 100029 China*

[c]*Ganjiang Innovation Academy Chinese Academy of Sciences Ganzhou 341000 China*

[d]*Dalian National Laboratory for Clean Energy Dalian 116023 China*

E-mail: zhuho128@126.com; qjchen@ipe.ac.cn

1. Experimental Section

1.1 Materials

Phytic acid solution (50% in H_2O), Aniline (AR, ≥99.5%), p-Phenylenediamine (99%), Manganese (II) chloride (AR, ≥99.0%), Chloroplatinic acid (AR, Pt≥37.5%) and isopropanol (AR, ≥99.5%) are purchased from Macklin Chemistry Co., Ltd. Ammonium persulphate (AR, ≥99.0%) is purchased from Aladdin Chemistry Co., Ltd. Nafion perfluorinated resin solution (5 wt%) in the experiment is obtained from Sigma-Aldrich Co., Ltd. All reagents are used directly and without further purification. Distilled deionized water was used throughout the experiments.

1.2 Morphological and structural characterization

X-ray diffraction (XRD) patterns of the supports and catalysts were recorded on a Rigaku, Japan, Smartlab (9) X-ray diffractometer using a CuKα source (λ=1.54056 Å) at 40 kV and 40 mA. A 2θ range from 5° to 90° was measured with a step size of 0.5° min-1. The phase composition and grain size of the prepared platinum catalyst were studied. The microcrystalline size was derived by the Scherrer equation. The half peak width (FWHM) of the platinum (111) peak was used for calculation. The samples were investigated by SEM with a SU8020 (HITACHI, Japan). TEM images were taken by a JEM-2100F instrument (JEOL, Japan). The samples were ultrasonically dispersed in ethanol and dropped onto a TEM grid. For characterization of the pore structure of the supports and catalysts, N_2 physisorption at 77 K were performed on an ASAP 2010 volumetric adsorption analyzer (Micromeritics, Norcross, USA). Prior to test, the samples were degassed at 80 °C for 10 h under vacuum. The BET specific surface area was determined in a relative pressure range of 0.05-0.2. The pore diameter was determined from the adsorption data. The Raman spectra were recorded with a Renishaw InVia Reflex micro-Raman system (Renishaw, Gloucestershire, UK) with a frequency He: Ne laser (633 nm) as excitation source. The laser power measured on the sample surface is 17 mW. The samples were investigated by SEM with a SU8020 (HITACHI, Japan). The XPS spectra were performed in ESCALAB 250Xi Versa Probe II spectrometer (Thermo Fisher Scientific, USA) using mono-chromated AlKα (1486.7 eV) X-ray radiation. All binding energies were referenced to the carbon 1s peak at 284.8 eV.

1.3 Electrochemical measurements for ORR

For the ORR at a RDE, the electron transfer number (n) and kinetic current density (J_K) were calculated from the Koutecky-Levich equation:

$$\frac{1}{J} = \frac{1}{J_L} + \frac{1}{J_K} = \frac{1}{B\omega^{\frac{1}{2}}} + \frac{1}{J_K}$$

$$B = 0.62nFC_0D_0^{\frac{2}{3}}V^{-\frac{1}{6}}$$

where J is the measured current density, J_K and J_L are the kinetic and limiting current densities, ω is the angular velocity of the disk, n is the electron transfer number, F is the Faraday constant (96485 C mol^{-1}), C_0 is the bulk concentration of O_2 (1.2×10^{-6} mol cm^{-3}), D_0 is the diffusion coefficient of O_2 ($1.9 \times 10\text{-}5$ cm^2 s^{-1}), and V is the kinematic viscosity of the electrolyte (0.01 cm^2 s^{-1}).

For RRDE tests, a Princeton applied research P3000A-DX electrochemical workstation was employed and the disk electrode was scanned catholically at a rate of 10 mV s^{-1} and the ring electrode potential was set to 1.40 V vs. RHE. The hydrogen peroxide yield (H_2O_2 %) and the electron transfer number (n) were determined by the following equations:

$$H_2O_2(\%) = 200 \times \frac{\frac{I_r}{N}}{I_d + \frac{I_r}{N}}$$

$$n = 4 \times \frac{I_d}{I_d + \frac{I_r}{N}}$$

Where I_d is the disk current, I_r is the ring current, and N = 0.4 is the current collection efficiency of the Pt ring.

2. Additional Material Characterizations

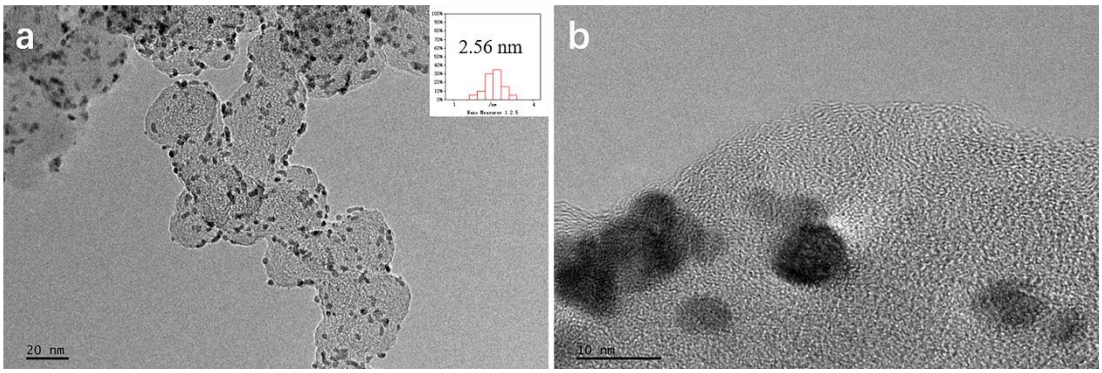

Fig. S1 (a) The HRTEM images of JM-Pt/C Catalyst (The insert in Fig. a is the corresponding particle size distribution), (b) Local magnification of JM-Pt/C catalyst.

Table S1 Por structure parameter of the CNF-1300, CNF-1300-0.28Mn and JM-Pt/C.

Sample	S_{BET}[a]	V_t[b]	D[c]
	$m^2\ g^{-1}$	$cm^3\ g^{-1}$	N_m
CNF-1300	482	0.56	8.6
CNF-1300-0.28Mn	565	0.69	11.6
JM-Pt/C	265	0.56	13.3

[a] BET specific surface area. [b] Total pore volume. [c] Average pore diameter calculated by adsorption curve.

Table S2 XPS results analysis for the prepared samples (at. %).

	Pt (at%)	C (at%)	N (at%)	O (at%)	Mn (at%)
Pt/CNF-900	3.63	76.98	6.07	13.31	-
Pt/CNF-1100	3.27	81.28	4.21	11.24	-
Pt/CNF-1300	2.96	86.97	2.92	7.16	-
Pt/CNF-1300-0.28Mn	2.69	89.84	2.12	5.14	0.21

Table S3 Information of C 1s for CNF, CNF-900, CNF-1100, CNF-1300 and CNF-1300-0.28Mn.

Sample	C-C (wt. %)	C=N (wt. %)	C-O-C (wt. %)	C-N (wt. %)	O-C=O (wt. %)
CNF	33.3	22.3	17.1	16.7	10.6
CNF-900	24.6	28.7	9.2	20.4	17.1
CNF-1100	33.4	27.2	0.0	25.0	14.4
CNF-1300	35.3	30.3	0.0	22.4	12.0
CNF-1300-0.28Mn	35.4	25.2	0.0	19.9	19.5

Table S4 Information of N 1s for CNF, CNF-900, CNF-1100, CNF-1300 and CNF-1300-0.28Mn.

Sample	Pyridinic-N (wt. %)	Pyrrolic-N (wt. %)	Graphitic-N (wt. %)	N-O (wt. %)
CNF	15.5	48.0	24.8	11.7
CNF-900	19.1	14.4	52.4	14.1
CNF1100	0.0	0.0	61.4	38.6
CNF1300	21.2	0.0	61.3	17.5
CNF-1300-0.28Mn	2.9	0.0	52.0	45.1

Table S5 Information of Pt 4f for Pt/CNF-900, Pt/CNF-1100, Pt/CNF-1300, Pt/CNF-1300-0.28Mn and JM-Pt/C.

	Pt^0 (at. %)	Pt^{2+} (at. %)
Pt/CNF-900	63.9	36.1
Pt/CNF-1100	74.8	25.2
Pt/CNF-1300	73.2	26.8
Pt/CNF-1300-0.28Mn	72.8	27.2
JM-Pt/C	64.2	35.8

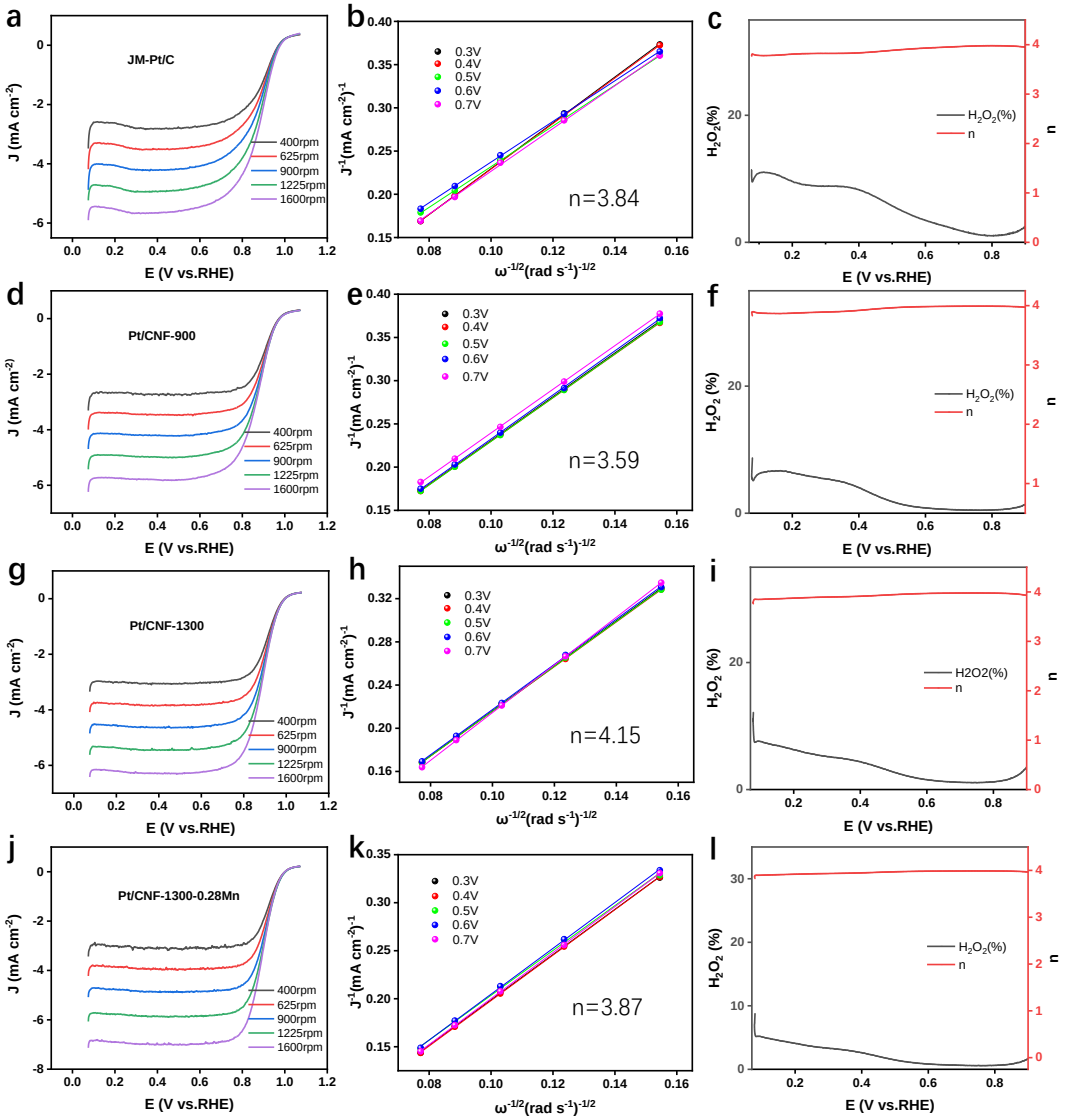

Fig. S2 ORR polarization curves in O_2-saturated 0.1M $HClO_4$ at various rotating sweeps, the corresponding Koutecky-Levich plots at different potentials and H_2O_2 yield and electron transfer number of (a-c) JM-Pt/C, (d-f) Pt/CNF-900, (g-i) Pt/CNF-1300 and (j-l) Pt/CNF-1300-0.28Mn.

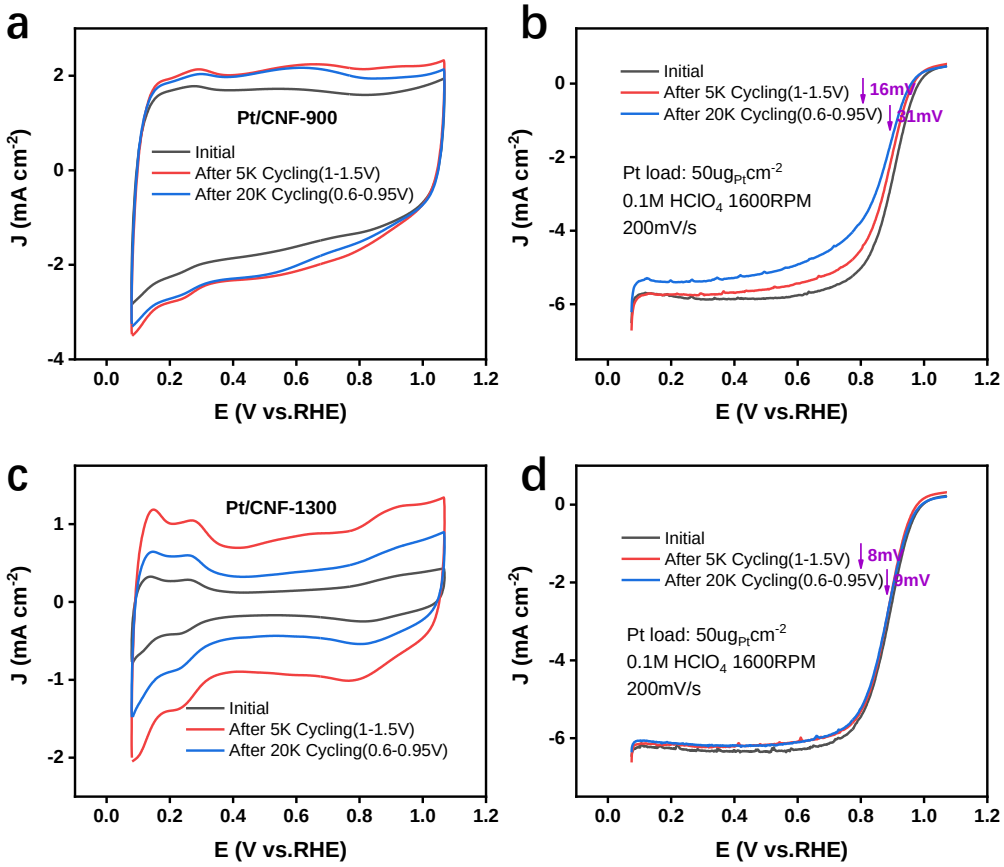

Fig. S3 Durability test of Pt/CNF-900 catalyst (a-b) and Pt/CNF-1300 catalyst (c-d) in a high potential range (1.0-1.5 V) and low potential range (0.6-0.95 V).

Table S6 Electrochemical results of different catalysts.

Sample	E_{onset} [a] (V)	$E_{1/2}$ (V)	J at 0.9 V (mA cm^{-2})
Pt/CNF-900	0.991	0.891	2.571
Pt/CNF-1100	0.992	0.893	2.941
Pt/CNF1300	1.002	0.891	2.957
Pt/CNF1400	1.003	0.810	0.861
JM-Pt/C	1.008	0.878	2.684
Pt/CNF-1300-0.05Mn	1.020	0.868	1.765
Pt/CNF-1300-0.28Mn	1.022	0.895	3.077
Pt/CNF-1300-0.42Mn	1.024	0.892	2.799

[a] Eonset refers to the overpotential at 0.1mA cm^{-2}.

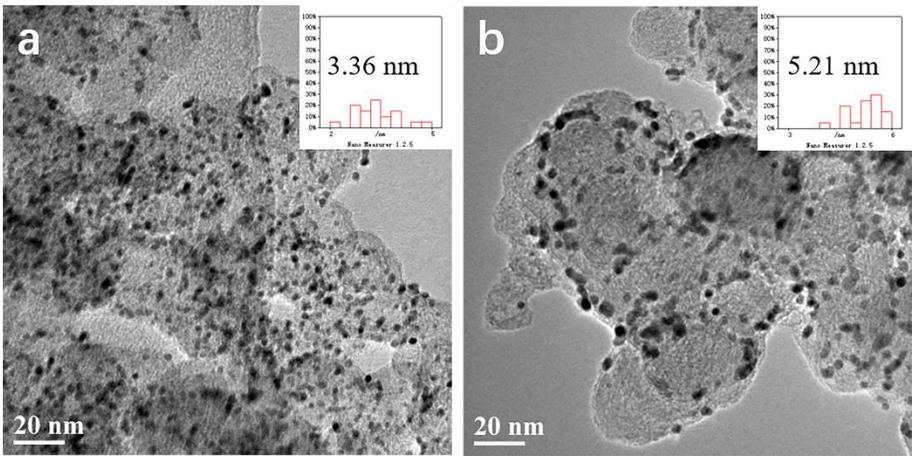

Fig.S4 The HRTEM images of JM-Pt/C Catalyst after (a) 5K and (b) 20K cycles. (The insert in Fig. a and b is the corresponding particle size distribution)